Research Paper

Deconvolving the pre-Himalayan Indian margin — Tales of crustal growth and destruction

Christopher J. Spencer [a,b,*], Brendan Dyck [c], Catherine M. Mottram [d,e], Nick M.W. Roberts [b], Wei-Hua Yao [a,f], Erin L. Martin [a]

[a] Earth Dynamics Research Group, The Institute for Geoscience Research (TIGeR), Department of Applied Geology, Curtin University, 6845, Perth, Australia
[b] NERC Isotope Geosciences Laboratory, British Geological Survey, Keyworth, Nottingham, NG12 5GG, UK
[c] Department of Earth Sciences, Simon Fraser University, University Drive, Burnaby V5A 1S6, Canada
[d] Department of Environment, Earth and Ecosystems, The Open University, Walton Hall, Milton Keynes, MK7 6AA, UK
[e] School of Earth and Environmental Sciences, University of Portsmouth, Portsmouth, PO1 3QL, UK
[f] Schoolof Earth Sciences and Engineering, SunYat-sen University, Guangzhou 510275, China

A B S T R A C T

The metamorphic core of the Himalaya is composed of Indian cratonic rocks with two distinct crustal affinities that are defined by radiogenic isotopic geochemistry and detrital zircon age spectra. One is derived predominantly from the Paleoproterozoic and Archean rocks of the Indian cratonic interior and is either represented as metamorphosed sedimentary rocks of the Lesser Himalayan Sequence (LHS) or as slices of the distal cratonic margin. The other is the Greater Himalayan Sequence (GHS) whose provenance is less clear and has an enigmatic affinity. Here we present new detrital zircon Hf analyses from LHS and GHS samples spanning over 1000 km along the orogen that respectively show a striking similarity in age spectra and Hf isotope ratios. Within the GHS, the zircon age populations at 2800—2500 Ma, 1800 Ma, 1000 Ma and 500 Ma can be ascribed to various Gondwanan source regions; however, a pervasive and dominant Tonianage population (∼860—800 Ma) with a variably enriched radiogenic Hf isotope signature (εHf = 10 to −20) has not been identified from Gondwana or peripheral accreted terranes. We suggest this detrital zircon age population was derived from a crustal province that was subsequently removed by tectonic erosion. Substantial geologic evidence exists from previous studies across the Himalaya supporting the Cambro-Ordovician Kurgiakh Orogeny. We propose the tectonic removal of Tonian lithosphere occurred prior to or during this Cambro-Ordovician episode of orogenesis in a similar scenario as is seen in the modern Andean and Indonesian orogenies, wherein tectonic processes have removed significant portions of the continental lithosphere in a relatively short amount of time. This model described herein of the pre-Himalayan northern margin of Greater India highlights the paucity of the geologic record associated with the growth of continental crust. Although the continental crust is the archive of Earth history, it is vital to recognize the ways in which preservation bias and destruction of continental crust informs geologic models.

© 2018, China University of Geosciences (Beijing) and Peking University. Production and hosting by Elsevier B.V. This is an open access article under the CC BY-NC-ND license (http://creativecommons.org/licenses/by-nc-nd/4.0/).

1. Introduction

Orogenic processes, both modern and ancient, drive the growth and destruction of continental crust (Scholl and von Huene, 2009; Spencer et al., 2017a). It is only with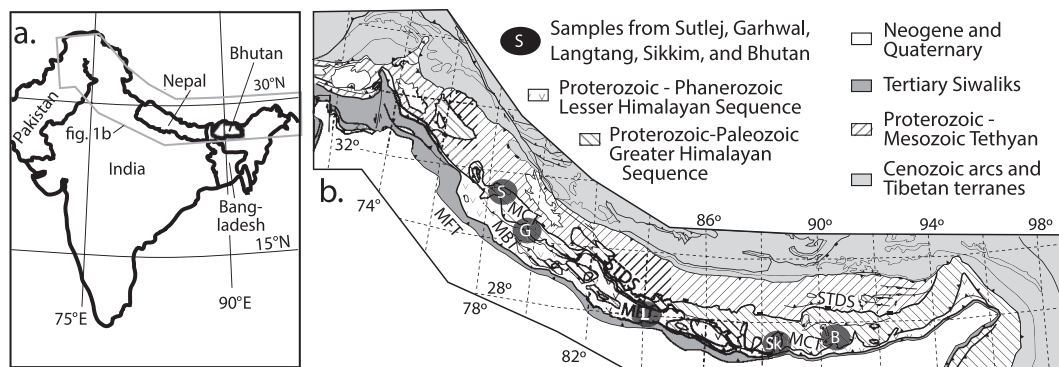in this continental crust that the deep history of the Earth can be extracted (Cawood et al., 2013). A large proportion of the continental crust is generally destroyed through tectonic processes operating within convergent margins that precede collisional orogenies (von Huene and Scholl, 1991; Scholl and von Huene, 2009; Stern, 2011).

Given the constructive and destructive nature of convergent margins (the Yin and Yang of subduction; Stern and Scholl, 2010; Roberts, 2012; Roberts and Spencer, 2015), the apparent peaks and troughs of zircon age frequency can be interpreted to represent the balance of crustal growth and removal (Hawkesworth et al.,

Figure 1. (a) Geographic map of the Himalaya. (b) Generalized tectonic map of the Himalayan orogen (after Kohn et al., 2010; Spencer et al., 2012a). Major fault systems include the South Tibetan detachment system (STDS), the Main Central thrust (MCT), the Main Boundary thrust (MBT), and the Main Frontal thrust (MFT). Detrital zircon samples from the GHS are marked in their respective regions (Sk: Sikkim, L: Langtang, G: Garhwal, S, Sutlej). Samples from this study are from the Langtang and Sikkim regions. Data from the Sutlej, Garhwal, and Bhutan regions are respectively reported by Richards et al. (2006), Spencer et al. (2012b), Hopkinson et al. (2017).

2009; Spencer et al., 2015). Crustal growth during an orogenic cycle forms a balance between magmatism (crustal growth) and tectonic removal (crustal loss) along subduction zones. Tectonic removal can form the mechanism by which crustal loss occurs, such as that identified along modern convergent margins (e.g. the Andes and Banda Arc; Kay et al., 2005; Tate et al., 2015). In ancient orogenic systems, detrital zircon preserved in distal sedimentary basins can provide important insights into the growth history of continental crust subsequently removed by tectonic processes along ancient convergent margins (Amato and Pavlis, 2010; Isozaki et al., 2010; Aoki et al., 2012).

The Cenozoic Himalayan Orogen is a classic example of collisional tectonic processes (Le Fort, 1986; Searle et al., 1987; Webb et al., 2007); however, the depth of geologic history represented in this mountain chain extends far beyond the most recent orogenic activity. It is likely the northern margin of India was previously the locus of multiple orogenic episodes extending into the Paleoproterozoic (Cawood et al., 2007; Kohn et al., 2010; Myrow et al., 2016). Although the Himalayan orogeny has overprinted the previous geologic history, detailed investigation of the sedimentary and igneous units that comprise the metamorphic core of the orogen offer useful insight into the pre-Himalayan history and provide key implications for how the continental record is preserved through geologic time.

We report Hf isotopes of detrital zircon from the metamorphic core across over 1000 km of the Himalaya that provide evidence for a major period of pre-Himalayan crustal destruction along the northern margin of Greater India, which further highlights the importance of applying the principles of uniformitarianism (i.e., subduction erosion in modern tectonic settings) to our tectonic models throughout geologic time.

2. Geologic setting

The Himalaya is often considered a quintessential example of a modern collisional orogeny (Fig. 1). Zircon geochronology has been a key tool in unraveling the geodynamics that preceded the Himalayan orogeny and the associated crustal architecture has been the focus of many studies (see e.g. DeCelles, 2000; Myrow et al., 2003; Gehrels et al., 2006; Cawood et al., 2007; Spencer et al., 2012a; Mottram et al., 2014), but large uncertainties remain for interpreting the pre-Himalayan tectonic history particularly in how sedimentary provenance is interpreted.

The Himalayan mountain front is comprised of three laterally continuous sedimentary packages deposited on the northern margin of Greater India (Gansser, 1964; Le Fort, 1975). The lower is

the Paleo- to Neoproterozoic Lesser Himalayan Sequence (LHS), which is overlain by the Neoproterozoic to Ordovician Greater and Tethyan Himalayan Sequence (GHS, THS) (Parrish and Hodges, 1996; Robinson et al., 2001; Myrow et al., 2003, Myrow et al., 2016). Analyses of Nd isotopes have shown that the GHS has a distinct geochemical signature from the LHS. The GHS has εNd values of −15 to −20 whereas the LHS has εNd of −20 to −25 (Parrish and Hodges, 1996; Ahmad et al., 2000; Robinson et al., 2001; Martin et al., 2005; Mottram et al., 2014).

Sample descriptions and U—Pb data from zircon analyzed for Hf in this study are reported in Mottram et al. (2014) and Dyck (2016). These new data are combined with previously published Hf zircon data from Richards et al. (2006) and Spencer et al. (2012b) (Fig. 1).

3. Methods and results

U—Pb geochronology of zircon was presented in the previous studies of Mottram et al. (2014) and Dyck (2016). Near concordant (>98% concordance) U—Pb zircon ablation sites from each of the samples were re-analyzed to measure their respective Lu—Hf isotopic compositions. Isotope analyses were carried out at NIGL using a Thermo Scientific Neptune Plus MC-ICP-MS coupled to a New Wave Research UP193FX excimer laser ablation system and low-volume ablation cell (Horstwood et al., 2003). Helium was used as the carrier gas through the ablation cell with Ar makeup gas being connected via a T-piece and sourced from a CetacAridus II desolvating nebulizer. After initial set-up and tuning the nebulizer air aspirated during the ablation analyses. Masses ^{172}Yb, ^{173}Yb, ^{175}Lu, ^{176}Hf + Yb + Lu, ^{177}Hf, ^{178}Hf, ^{179}Hf, and ^{180}Hf were measured simultaneously during static 30-s ablation analyses with a 35 μm diameter spot and a fluence of 8–10 J/cm^2.

Reference zircons Mudtank and 91500 were used to monitor accuracy and precision of internally corrected (using ^{179}Hf/^{177}Hf = 0.7325) Hf isotope ratios and instrumental drift with respect to the Lu/Hf ratio. Hf reference solution JMC475 was analyzed during each analytical session to allow normalization of the fundamental mass spectrometer performance. JMC475 doped with 2 ppb Yb was also run during each session to monitor the efficacy of the ^{176}Yb interference correction on ^{176}Hf. A ^{176}Yb/^{173}Yb = 0.79448 was used for this correction. This ratio was determined using Yb-doped JMC475 and corrected for mass bias using ^{179}Hf/^{177}Hf. In this way, the determined Yb ratio is a 'true' Yb ratio calibrated for the mass bias difference between Hf and Yb (cf. Nowell and Parrish, 2001). This correction mechanism relies on the previously determined calibration to still be valid during the run session. This is demonstrated by the running of validation materials
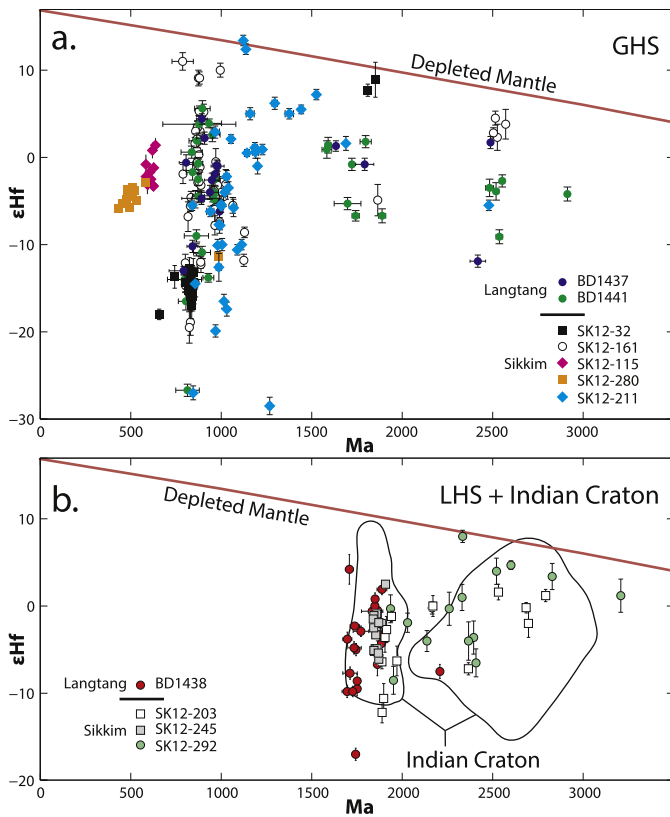
Figure 2. Plots of new εHf data of zircon from the (a) GHS of the Langtang and Sikkim regions and (b) LHS and Indian cratonic basement from the same (U–Pb data from Mottram et al., 2014 and Dyck, 2016). Fields outlining the range of ages and εHf values of the Indian craton are from Kaur et al. (2011).

91500 and Mud Tank reference materials. ^{176}Lu interference on the ^{176}Hf peak was corrected by using the measured ^{175}Lu and assuming ^{176}Lu/^{175}Lu = 0.02653. Sample results are provided in Supplementary Table 1.

Systematic uncertainties of ^{176}Hf/^{177}Hf and ^{176}Lu/^{177}Hf isotope ratios were propagated using quadratic addition, incorporating the external variance of the reference material during each analytical session. Reference zircon 91500 was used to normalize the ^{176}Lu/^{177}Hf ratio assuming ^{176}Lu/^{177}Hf = 0.000288 (Woodhead et al., 2004) with a minimum uncertainty of 10% (2 standard deviations). The uncertainty propagation of the epsilon notation also includes the uncertainty of the ^{207}Pb/^{206}Pb crystallization age and the Lu/Hf

analysis, as it is time integrated. Although this could over-estimate the uncertainty, we prefer this conservative approach for the epsilon notation when defining specific fields of similar εHf compositions. For instance, incorporating crystallization age uncertainty produces estimates that are 50% larger, on average, than estimates that do not consider crystallization age and Lu/Hf uncertainty.

Results of Hf analyses over nine sessions spanning three weeks for reference zircons 91500 and Mudtank zircon are presented in the inline supplementary table and figure. Hf ratios of Mudtank are self-normalized so only precision is of relevance here. See online Supplementary Table 1 for reference material results and full data tables.

The results of these new Hf analyses are presented in supplementary materials and Fig. 2. The individual samples from Sikkim and Langtang (Fig. 1) reveal strikingly similar εHf signatures in each of the age populations (see Fig. 2). Importantly, the Tonian age population in both localities display significant radiogenic Hf enrichment, with $\varepsilon_{Hf}(t)$ values as low as −28.

To visualize the U–Pb and Hf data distribution and density, we employ bivariate kernel density estimation (2dKDE). This method uses kernel density estimation (Botev et al., 2010) with discrete bandwidths for both the x- and y-axes (20 Ma and 1 epsilon, respectively). The Matlab script for this procedure is available upon request to the corresponding author. An example of 2dKDE using U–Pb and εHf data from the GHS are displayed in Fig. 3. To simplify the distribution, we extract the contours that correspond to 10th, 50th, and 90th percentile of the data. This method is used to compare distributions between the various regions discussed in this study.

4. Discussion

4.1. Provenance of the LHS

Detrital zircon analyses of the metasedimentary rocks of the LHS and slivers of Indian cratonic basement across the Himalaya reveal a dominant Paleoproterozoic age population with variable amounts of Archean age zircon (Fig. 2; Martin et al., 2005; McQuarrie et al., 2008; Kohn et al., 2010; Gehrels et al., 2011; Spencer et al., 2012b; Mottram et al., 2014; Dyck, 2016). This is consistent with a derivation from the proximal crustal blocks of cratonic India (Spencer et al., 2012b).

4.2. Provenance of the GHS

Recent detrital zircon studies have identified similar age spectra with a dominant Tonian age peak in Sutlej (e.g. Martin
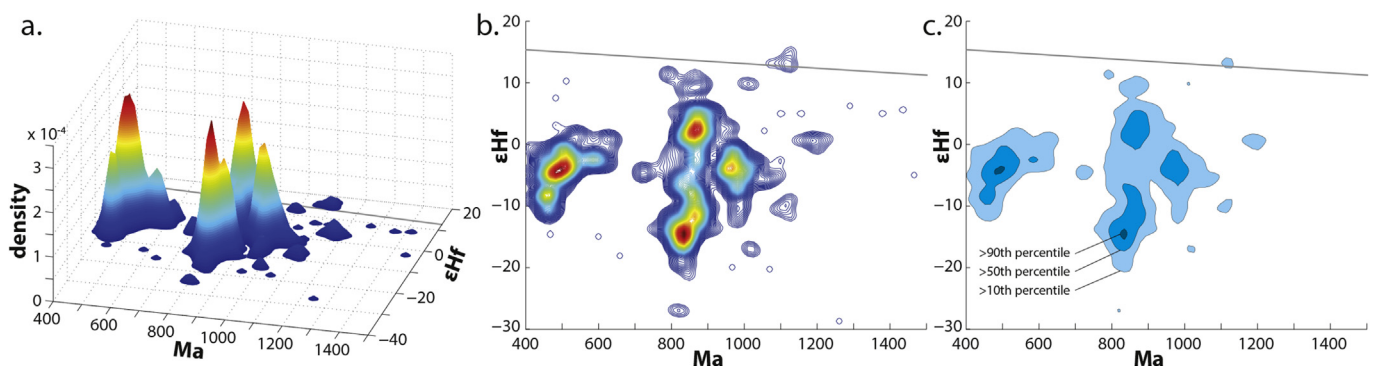
Figure 3. (a) Oblique view of bivariate kernel density estimation (2dKDE; after Botev et al., 2010) of the GHS εHf data. (b) Azimuthal view of 2dKDE. (c) Simplified 2dKDE with only the contours corresponding to 90th, 50th, 10th percentile showing.

et al., 2005), Garhwal (e.g. Spencer et al., 2012b), Nepal (e.g. Gehrels et al., 2011; Dyck, 2016) and as far to the east as Sikkim (e.g. Mottram et al., 2014), Bhutan (e.g. Yin et al., 2010; McQuarrie et al., 2013; Webb et al., 2013), and Arunachal (DeCelles et al., 2009). Myrow et al. (2003, 2010, 2016) also report detrital zircon age spectra from an array of Cambrian sil-iciclastic units across the Tethyan Himalaya many of which display dominant age peaks between ~750 Ma and 900 Ma. Additionally, Hopkinson et al. (2017) reported inherited zircon in leucogranite intruding the GHS in Bhutan with similar age and isotopic information as those presented in this study. Given the protracted magmatic record of Gondwana, identifying the depositional provenance of the GHS provides many non-unique scenarios and thus makes it difficult (if not impossible) to reconstruct depositional provenance using U–Pb ages alone. Hf isotopes provide an additional discrimination tool for recon-structing the tectono-sedimentary evolution of this region. In the following section, we first outline the potential source regions of the various regions within the core of Gondwana (Collins and Pisarevsky, 2005) and second of the crustal blocks peripheral to Gondwana (including the South China Craton).

4.2.1. Arabian Nubian Shield

The first depositional provenance study using zircon posited that the Arabian Nubian Shield was a likely source region of the enigmatic Tonian zircon age population (DeCelles, 2000). Since then, thousands of zircon U–Pb and Hf analyses from the basement rocks of the ANS and detrital zircon derived there from display a tight range of εHf during the time period in question, with the 90th percentile of the data ranging from +13 to +2 (Fig. 4a) (Be'eri-Shlevin et al., 2010; Morag et al., 2011, 2012; Ali et al., 2012, 2013, 2014, 2015a,b,c; Be'eri-Shlevin et al., 2013; Iizuka et al., 2013a,b; Robinson et al., 2014). This is in contrast to zircon Hf from the GHS (Fig. 3), in which the 90th percentile of the data range from +13 to −22. A direct comparison between these εHf pop-ulations (Fig. 4a) displays the dramatic difference between these two regions. Furthermore, the absence of a dominant ~600 Ma population in the GHS which are present in the ANS further argues against derivation there from as the depositional ages of the GHS, and its equivalents (the outer LHS of Myrow et al., 2003; Martin et al., 2005; McQuarrie et al., 2008) are Cambrian or latest Neo-proterozoic (Long and McQuarrie, 2010; Gehrels et al., 2011; Spencer et al., 2012b; Dyck, 2016).

4.2.2. East African Orogen

Zircon εHf data from the East African Orogen are from Madagascar, Mozambique, and Ethiopia (Thomas et al., 2010; Archibald et al., 2015; Blades et al., 2015). These data come from various sedimentary successions deposited in proximal and conti-nental fluvial environments as well as felsic igneous rocks attrib-uted to subduction and/or collisional magmatism. The data cluster at ca. 7 epsilon at ~1060 Ma, with a bimodal ~720–860 Ma population at ca. −25 to −5 epsilon and ca. −7 epsilon, and a spread of ~650–500 Ma data between ca. 10 and −30 epsilon (Fig. 4b). While there is overlap between the ~860 Ma GHS population with enriched Hf, there is a clear mismatch, with the largest proportions of the εHf data in the East African Orogen. Additionally, there is no significant overlap in the Paleozoic zircon populations between the East African Orogen and the GHS.

4.2.3. Antarctica

Zircon εHf from Antarctica (Fig. 4c) reveal major Cryogenian-Ediacaran zircon populations and a broad scatter of data through the Mesoproterozoic–Tonian (Veevers and Saeed, 2008; 2011; Zhang et al., 2012; Yakymchuk et al., 2015). Two major

Neoproterozoic orogens associated with Gondwana assembly are located within Antarctica, the Kuunga Orogen, and the Terra Aus-tralis Orogen. Timing of the initiation of Terra Australis magmatism along the eastern margin of Antarctica is debated (Cawood, 2005), but thought to have commenced ca. 570 Ma and certainly not before ca. 630 Ma when passive margin sequences were deposited (Goodge, 1997; Vaughan and Pankhurst, 2008; Boger, 2011). While the εHf data from the GHS and Antarctica are similar at ca. 550–500 Ma and εHf = −5 (Fig. 4c), it is unlikely that the source of the zircon in the GHS is the Antarctic Terra Australis Orogen, as detritus would have been required to cross major orogenic boundaries (the Kuunga and possibly East African Orogens) to travel from source to sink. The similarity between the GHS and Antarctica post ~700 Ma may be symptomatic of Northern India and East Antarctica being part of the same convergent margin at the periphery of Gondwana when the supercontinent (Martin et al., 2017).

Neoproterozoic orogenesis in western Antarctica – the Kuunga-Pinjarra orogeny associated with the collision of India with Antarctica and Australia, may have shed detritus to the GHS. There is some overlap between the Tonian εHf signature from Antarctica and the GHS and magmatic rocks (ca. 930–900 Ma) of the Grove Mountains, the latter being part of the Kuunga-Pinjarra orogeny. This is likely to be the source of this zircon population in Antarctica. However, orogenesis in this region is characterized by distinct pulses of magmatism and metamorphism at ca. 900 Ma and 500 Ma, and thus cannot be attributed to <900 Ma zircon within the Antarctic population. The >10th percentile contour at ca. 850 Ma and εHf of −15 in the GHS data is not reflected in the Antarctic data, and so Antarctica is unlikely to be a unique source for the GHS detritus.

4.2.4. Australia

The Tonian is not a period associated with arc magmatism in Australia, but rather one of rifting and passive margin develop-ment. Following major pre-, syn- and post-collisional magmatism in the Mesoproterozoic, particularly in the Albany-Fraser and Musgrave orogens of south and central Australia, the early Neo-proterozoic is characterized by the development of major sedi-mentary basins in the central and northwestern regions, and the emplacement of dykes and sills along the eastern margin associated with the protracted breakup of Rodina (e.g. Walter et al., 1995; Maidment et al., 2007). In northwestern Australia, magmatism and transpressional deformation, arguably associated with a conver-gent plate margin (Martin et al., 2017), commenced with the ca. 750–530 Ma Paterson-Petermann Orogen. This is reflected by >90th percentile and >50th percentile εHf density contours from ca. 700–550 Ma in the NW Australia dataset (Fig. 4d). Northwest Australia and Northern India have been directly correlated along the Gondwana margin during the latest Neoproterozoic–Cambrian, which is reflected by the similar εHf values between the GHS and NW Australia zircon data ca. 650 Ma (Fig. 4d). However, prior to this, there is not a strong correlation in the data. There is a match between the more depleted components of the GHS and NW Australia data from ca. 1000–800 Ma, suggesting a possible shared source for the detritus. However, the Tonian GHS data show the >10th percentile density contour at εHf = −15, which is not recorded by the data from Northern Australia; thus, the source of GHS cannot be solely attributed to NW Australia.

4.2.5. Cathaysia

The Cathaysia Block of the South China craton, which is thought to have been located off the northern Indian margin of Gondwana (Yao et al., 2014a,b), is another likely source region of the GHS because the two shared a common ~980 Ma zircon age population in their coeval late-Neoproterozoic to early-Paleozoic sedimentary
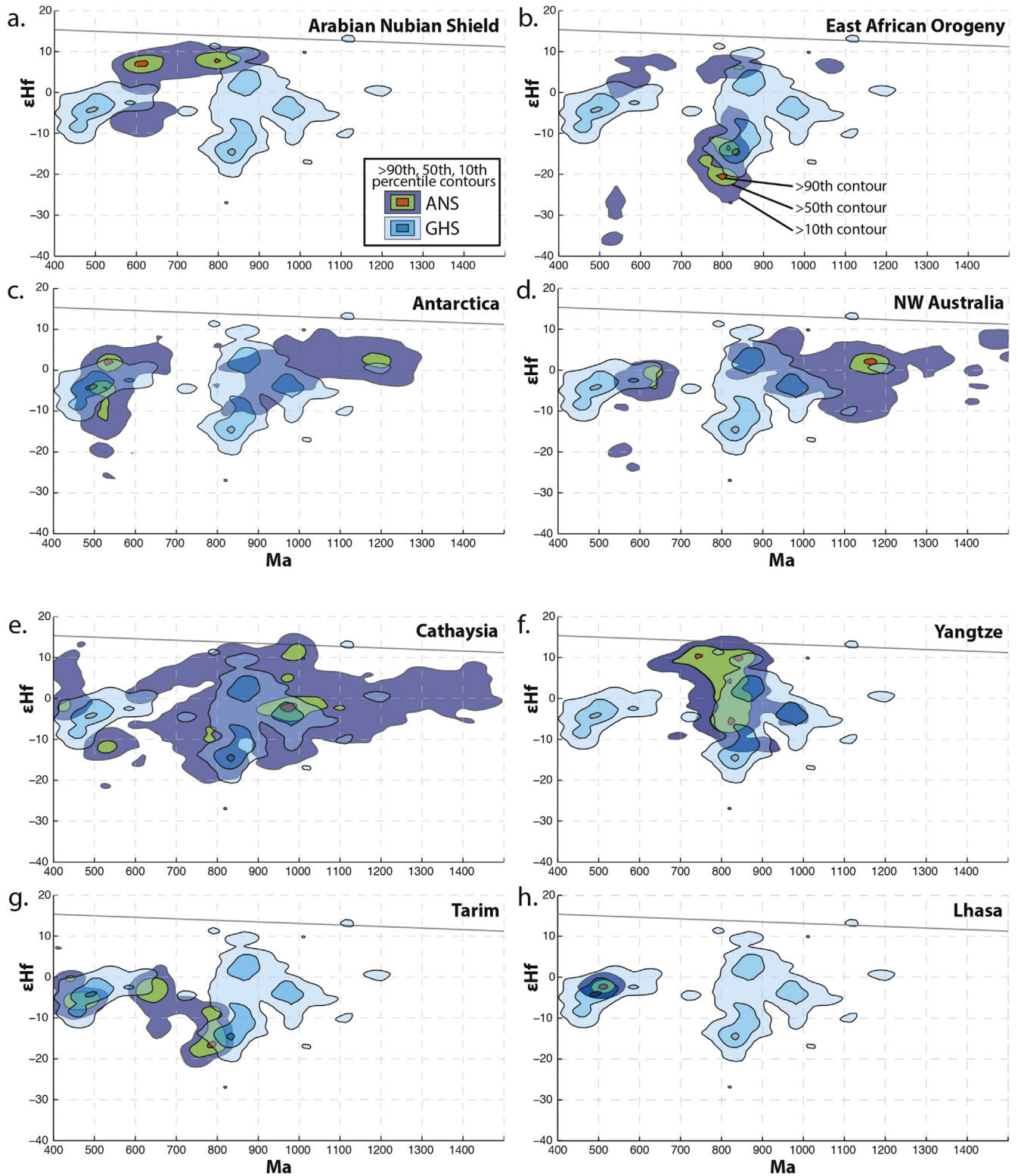
Figure 4. (a) 2dKDE of the GHS compared with the Arabian Nubian Shield (Be'eri Shlevin et al., 2010, 2013; Morag et al., 2011, 2012; Ali et al., 2012, 2013, 2014, 2015a,b,c; Iizuka et al., 2013a,b; Robinson et al., 2014). (b) 2dKDE of the GHS compared with the East African Orogeny (Thomas et al., 2010; Archibald et al., 2015; Blades et al., 2015). (c) 2dKDE of the GHS compared with Antarctica (Veevers and Saeed, 2008, 2011; Zhang et al., 2012; Yakymchuk et al., 2015). (d) 2dKDE of the GHS compared with northwest Australia (Martin et al., 2017). (e) 2dKDE of the GHS compared with the Cathaysia block (Yu et al., 2008, 2010, 2012, 2017; Li et al., 2011; Shu et al., 2011; Yao et al., 2011; Li et al., 2012a; Li et al., 2012b; Wang et al., 2013a, b; Yao et al., 2014a,b; Cui et al., 2015; Wang et al., 2015; Wang et al., 2015b; Yan et al., 2015; Shen et al., 2016; Chen et al., 2017; Zou et al., 2017). (f) 2dKDE of the GHS compared with the Yangtze block (Huang et al., 2008; Yu et al., 2008; Zhou et al., 2009; Wang et al., 2012; Chen et al., 2016; Yao et al., 2016; Su et al., 2017; Wang et al., 2017). (g) 2dKDE of the GHS compared with the Tarim block (Long et al., 2011; Ge et al., 2012; Song et al., 2013). (h) 2dKDE of the GHS compared with the Lhasa block (Hu et al., 2013; Ding et al., 2015).

rocks (Yao et al., 2014a,b, 2015). The Cathaysia Block further preserved massive 850−725 Ma bimodal magmatic and volcanoclastic rocks (Li et al., 2005, 2008, 2010; Wang et al., 2010a,b, 2012), which could have possibly fed Tonian zircon to the GHS. The compiled detrital zircon data from the Cathaysia late-Neoproterozoic to early-Paleozoic sediments exhibit a wide range of εHf values, in which the 10th percentile contour ranges from ∼15 to −20, covering the zircon εHf range of the GHS (Fig. 4e). However, the 90th percentile εHf data at the late-Tonian age cluster (εHf of −1 to −3) of the GHS does not match the data from Cathaysia (Fig. 4e). The early-Tonian populations are similar between the GHS and Cathaysia, implying a possible provenance linkage, but only prior to ∼900 Ma. Taking into consideration the paleo-topography likely excludes Cathaysia to be a source region for the GHS, as the sedimentological data point to all of Cathaysia being submerged during the late-Neoproterozoic, and thus it cannot serve as a siliciclastic erosion zone (Liu and Xu, 1994; Yao et al., 2014a,b). Furthermore, the wide range of post-800 Ma detrital zircon ages with radiogenic Hf unique to the Cathaysia block and without indigenous sources implies an exotic source. The εHf similarities of the early-Tonian zircon between the GHS and the Cathaysia, therefore, allow for a common detrital source from a third party.

4.2.6. Yangtze

The Yangtze Block, on the other side of the South China craton from the Cathaysia Block, also records massive 850−725 Ma magmatic rocks (e.g., Zhou et al., 2006; Wang et al., 2008), of which the Tonian-Cryogenian zircon were recycled and preserved in Neoproterozoic sediments (Fig. 4f). To account for the Yangtze as the possible source region of the GHS, we compare the zircon εHf contour plots of the two regions. The 50th percentile concentrates of the Yangtze data ranges from ∼15 to −12 (Fig. 4f), whereas the 50th percentile GHS data range is separated into two fields (∼6 to −1, and −7 to −19). Furthermore, neither age populations nor εHf values of the 10th percentile overlap between of the two datasets. It is thus concluded that the Yangtze block also can be discounted as providing detrital zircon to the GHS during the late-Neoproterozoic period.

4.2.7. Tarim

Tarim is another Asian block located on the peripheral margin of eastern Gondwana, close to north Australia (Han et al., 2015). The Tarim Block experienced intensive 800−750 Ma and ∼650 Ma magmatic events that involved contrasting crustal components, with the 800−750 Ma magmatism yielding a εHf range of −22 to −4 (Long et al., 2011), and with the ∼650 Ma magmatism with more depleted εHf that range from −15 to +5 (Ge et al., 2012). Comparison between the Tarim Block and GHS (Fig. 4g) clearly display that the Tarim Block was not the source region to the GHS. Additionally, a 1000−950 Ma zircon population is absent in the Tarim sedimentary units. This contrasts with a vital component of the GHS sediments, and further supports the mismatch of the two in the Neoproterozoic history of magmatism, sedimentation, and crustal growth (Fig. 4g).

4.2.8. Lhasa

The Lhasa terrane lies north of the Tethyan Himalaya in the Tibetan Plateau and was the last continental block to collide with Eurasia before India's collision in the Cenozoic (Metcalfe, 2009). Latest Neoproterozoic to Cambrian volcanism in the central Lhasa Terrane has been attributed to the development of an Andean-type arc system along the proto-Tethyan margin of Gondwana (Zhu et al., 2012; Ding et al., 2015). While the exact location of the Lhasa terrane on the proto-Tethyan margin of Gondwana is debated (e.g. Zhu et al., 2011; Zhang et al., 2014), the match of the εHf data between the GHS and the Lhasa terrane at ca. 500 Ma appears to suggest that these two candidates may have shared a common zircon source.
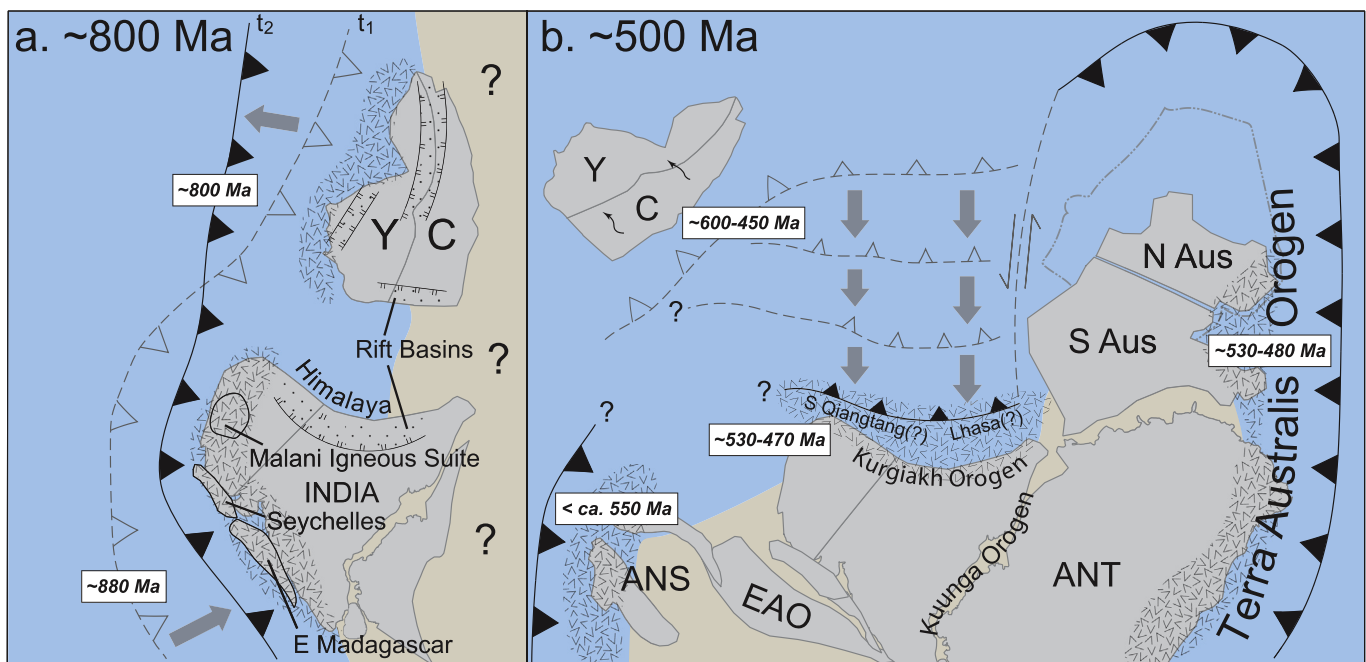
Figure 5. Paleogeographic reconstructions at (a) ∼800 Ma (after Cawood et al., 2017; Merdith et al., 2017) and (b) ∼500 Ma (after Merdith et al., 2017). See text for details. Positions of Neoproterozoic rift basins after Wang and Li (2003) and Mottram et al. (2014). Y: Yangtze, C: Cathaysia, EAO: East African Orogeny, ANS: Arabian Nubian Shield, ANT: Antarctica, S and N Aus: South and North Australia.

5. Paleogeography and tectonic model

While we acknowledge the importance of paleomagnetic data in constraining the paleogeography of tectonic models. Paleomagnetism and geology often provide non-unique solutions to paleogeography where multiple reconstructions are permissible given the empirical constraints (Merdith et al., 2017). In Fig. 5, plate reconstructions, which satisfy the paleomagnetic constraints (after Cawood et al., 2017; Merdith et al., 2017), are presented for ∼800 Ma and ∼500 Ma. Based upon the εHf data from Yangtze and India, we propose that the middle Tonian Period (∼800 Ma, Fig. 5a) was characterized by a retreating subduction zone along the Yangtze margin and advancing subduction along the eastern Indian margin. εHf data from the GHS of India display a time-progressive radiogenic enrichment from ∼880 to ∼840 Ma consistent with greater continental reworking. The lack of necessary source rocks for these ∼880 to ∼840 Ma zircons with radiogenically enriched Hf along the proposed eastern India convergent margin may indicate the potential of tectonic erosion of this source material driven by advancing subduction. In contrast, the Yangtze displays increasingly depleted εHf from ∼840 Ma to ∼700 Ma (Fig. 4f) indicative of greater mantle input. This subduction scenario is also consistent with the arc-derived sediments in the Nanhua sedimentary successions (Wang et al., 2012; Wang and Zhou, 2012).

The Cambrian Gondwana was characterized by a near-circum-Gondwana subduction zone with the Terra-Australis Orogen along the margins of Australia, Antartica, and South America (Cawood, 2005), along with the interior subduction/collision system of the East African Orogen between east Africa, Antarctica, and India (Collins and Pisarevsky, 2005). The tectonic history of the northern margin of Gondwana has been the subject of much debate regarding the specific positions of various continental blocks/terranes including Turkey, Iran, Lhasa, southern Qiangtang, Sibumasu, and Burma (see Hu et al., 2015 for review). While the late-Neoproterozoic to Cambro-Ordovician magmatism of each block displays unique isotopic signatures (Fig. 4), there is a general decrease in magmatic ages from west to east starting at ∼550 Ma in Turkey (Gürsu and Göncüoglu, 2005) and progressing through Iran (Hassanzadeh et al., 2008) to India, where it terminates at ∼470 Ma (Spencer et al., 2012b; Hu et al., 2015). Western Australia, on the other hand, displays magmatism associated with the Paterson-Petermann Orogen which was active from ∼680 Ma to ∼600 Ma, with transpression continuing until ∼530 Ma (Martin et al., 2017). Zircon crystallization in the Leeuwin Complex in southwest Australia is also older than that of adjacent India which ceases ∼500 Ma (Collins, 2003).

The timing of deformation within the Kurgiakh Orogeny (also referred to as the Bhimphedian Orogeny; Cawood et al., 2007) along the northern margin of India is constrained between ∼495 Ma and ∼460 Ma based upon biostratigraphy of pre- and post-orogenic granite and sedimentary successions (Gehrels et al., 2006; Myrow et al., 2016). Importantly, magmatism preserved in India and the adjacent Lhasa and Qiangtang blocks predate the deformation phase of the Kurgiakh Orogeny by over 30 million years (Lee and Whitehouse, 2007; Guynn et al., 2012; Pan et al., 2012). We posit the distinct break in the progression of magmatic ages along the northern margin of Gondwana. The protracted nature of magmatism associated with the Kurgiakh Orogeny may indicate the advancement and accretion of an oceanic arc complex (comprising the Lhasa and southern Qiangtang blocks along with pre-ca. 500 Ma arc-related rocks in the GHS) onto the northern margin of India. This protracted phase of magmatism may have accommodated by the presence of a continental-scale strike-slip fault system allowing

convergence to proceed for a greater period of time than of the adjacent Western Australia.

Although not the main focus of this paper, the Hf comparison diagrams (Fig. 4) point to the potential of an outboard arc system with a more depleted εHf signature fringing the Cathaysia-side of the South China Block post-800 Ma. While most of South China was submerged during the Ediacaran to Cambrian time, the presence of Neoproterozoic detritus for which no equivalents can be found within either South China itself or the environs of Gondwana provides the potential for a fringing arc system outboard of the Cathaysia coast (Fig. 5). The absence of such an arc system in the geological record may indicate this arc has also been tectonically eroded leaving behind only the eroded remnants.

6. Crustal destruction

Along modern active margins such as the Andes, the subducting plate may tectonically erode the upper plate and carry that material into the mantle (von Huene and Scholl, 1991; Clift and Vannucchi, 2004; Stern, 2011). Similarly, along the arc-continent collision occurring between the Banda Arc and northern Australia, a large swath of the Australian continent has been subducted beneath the Banda Arc (Spakman and Hall, 2010). The presumption of tectonic removal throughout geologic history implies the modern detrital zircon record is a function of crustal destruction by tectonic processes and preservation by continental collision (see Hawkesworth et al., 2009; Spencer et al., 2015). Roberts and Spencer (2015) further posited that this supercontinent-dominated destruction/preservation relationship is present in the geologic record back to the beginning of the Proterozoic Eon.

We postulate that the dominant Tonian detrital zircon age population present across the entire length of the GHS was sourced from an active continental margin that fringed the northern margin of India, which was subsequently removed via tectonic processes prior to the accretion of Asian continental fragments during the Kurgiakh Orogeny (Fig. 5b). The vestiges of this magmatism are currently seen in few places along the Himalaya, such as the Tonianaugen gneisses in Sikkim (Mottram et al., 2014) and Bhutan (Thimm et al., 1999), or in the Lesser Himalayan Granite Belt (LHGB) such as the Chor granitoid (Singh et al., 2002). It is possible that other magmatic bodies exist in the GHS or LHGB, and that have been previously assumed to belong to the Cambrian−Ordovician granites and orthogneisses that are similar in appearance (Singh et al., 2002). Nevertheless, the presence of Tonian age zircon population with an enriched Hf signature across the entire Himalayan orogen as far west as the Garhwal Region (Spencer et al., 2012b) and as far east as Bhutan (Hopkinson et al., 2017), gives further evidence that affinity from an uncharacterized source in the regions to the west or east of the Himalaya (e.g. Afghanistan or Indochina) is unlikely.

7. Conclusions

The results presented here are used to infer the presence of an active convergent margin along the northern margin of India responsible for the formation of Tonian continental crust now recorded in the detrital record of the GHS. This active margin was subsequently consumed by tectonic processes culminating in the Cambro-Ordovician Kurgiakh Orogeny.

As stated by Keppie et al. (2009), "When geological candidates for the missing material cannot be identified elsewhere, tectonic processes must be considered" (von Huene and Scholl, 1991; Clift and Vannucchi, 2004). It is clear from the tectonics

of Cenozoic convergent margins that tectonic processes play a major role in shaping the continental margins both in terms of crustal growth as well as crustal recycling. This is a principle that is rarely, and in most cases rightfully so, not applied in ancient orogenic systems. In the case of the Tonian detrital zircon age population with radiogenically enriched Hf in the GHS, until some other Gondwanan source is discovered and proposed as the source region of this material, we hypothesize that tectonic processes have removed the crust from which these zircon were derived.

Acknowledgements

Appendix A. Supplementary data

Supplementary data related to this article can be found at https://doi.org/10.1016/j.gsf.2018.02.007.

Inline supplementary figure 1: Hf isotope data from zircon reference materials. Reference values for Mudtank, 91500, and Plesovice are from Woodhead and Hergt (2005), Griffin et al. (2006), Sláma et al. (2008), respectively. Data visualization made with KDX (Spencer et al., 2017b).

References

Ahmad, T., Harris, N., Bickle, M., Chapman, H., Bunbury, J., Prince, C., 2000. Isotopic constraints on the structural relationships between the lesser Himalayan series and the high Himalayan crystalline series, Garhwal Himalaya. Geological Society of America Bulletin 112 (3), 467–477.

Ali, K.A., Andersen, A., Manton, W.I., Stern, R.J., Omar, S.A., Maurice, A.E., 2012. U–Pb zircon dating and Sr–Nd–Hf isotopic evidence to support a juvenile origin of the ~ 634 Ma El Shalul granitic gneiss dome, Arabian–Nubian Shield. Geological Magazine 149, 783–797.

Ali, K.A., Jeon, H., Andresen, A., Li, S.-Q., Harbi, H.M., Hegner, E., 2014. U–Pb zircon geochronology and Nd–Hf–O isotopic systematics of the Neoproterozoic HadbadhDayheen ring complex, Central Arabian Shield, Saudi Arabia. Lithos 206–207, 348–360. https://doi.org/10.1016/j.lithos.2014.07.030.

Ali, K.A., Kröner, A., Hegner, E., Wong, J., Li, S.-Q.Q., Gahlan, H.A., Abu El Ela, F.F., 2015a. U–Pb zircon geochronology and Hf–Nd isotopic systematics of Wadi-Beitan granitoid gneisses, South Eastern Desert, Egypt. Gondwana Research 27, 811–824. https://doi.org/10.1016/j.gr.2013.11.002.

Ali, K.A., Surour, A.A., Whitehouse, M.J., Andresen, A., 2015b. Single zircon Hf–O isotope constraints on the origin of A-type granites from the Jabal Al-Hassir ring complex, Saudi Arabia. Precambrian Research 256, 131–147. https://doi.org/10.1016/j.precamres.2014.11.007.

Ali, K.A., Wilde, S.A., Stern, R.J., Moghazi, A.-K.M., Ameen, S.M.M., 2013. Hf isotopic composition of single zircons from Neoproterozoic arc volcanics and post-collision granites, Eastern Desert of Egypt: implications for crustal growth and recycling in the Arabian-Nubian Shield. Precambrian Research 239, 42–55.

Ali, K.A., Zoheir, B.A., Stern, R.J., Andresen, A., Whitehouse, M.J., Bishara, W.W., 2015c. Lu—Hf and O isotopic compositions on single zircons from the North Eastern Desert of Egypt, Arabian–Nubian Shield: implications for crustal evolution. Gondwana Research. https://doi.org/10.1016/j.gr.2015.02.008.

Amato, J.M., Pavlis, T.L., 2010. Detrital zircon ages from the Chugach terrane, Southern Alaska, reveal multiple episodes of accretion and erosion in a sub-duction complex. Geology 38 (5), 459–462.

Aoki, Kazumasa, et al., 2012. Tectonic erosion in a Pacific-type orogen: detrital zircon response to cretaceous tectonics in Japan. Geology 40 (12), 1087–1090.

Be'eri-Shlevin, Y., Katzir, Y., Blichert-Toft, J., Kleinhanns, I.C., Whitehouse, M.J., 2010. Nd–Sr–Hf–O isotope provinciality in the northernmost Arabian–Nubian Shield: implications for crustal evolution. Contributions to Mineralogy and Petrology 160, 181–201.

Be'eri-Shlevin, Y., Avigad, D., Gerdes, A., Zlatkin, O., 2013. Detrital zircon U-Pb-Hf systematics of Israeli coastal sands: new perspectives on the provenance of Nile sediments. Journal of the Geological Society 171 (1), 107–116. https://doi.org/10.1144/jgs2012-151.

Blades, M.L., Collins, A.S., Foden, J., Payne, J.L., Xu, X., Alemu, T., Woldetinsae, G., Clark, C., Taylor, R.J.M., 2015. Age and hafnium isotopic evolution of the Didesa and Kemashi Domains, western Ethiopia. Precambrian Research 270, 267–284.

Botev, Z.I., Grotowski, J.F., Kroese, D.P., 2010. Kernel density estimation via diffusion. Annals of Statistics 38 (5), 2916–2957.

Cawood, P.A., Johnson, M.R.W., Nemchin, A.A., 2007. Early palaeozoic orogenesis along the indian margin of Gondwana: tectonic response to Gondwana assembly. Earth and Planetary Science Letters 255 (1–2), 70–84. https://doi.org/10.1016/j.epsl.2006.12.006.

Cawood, P.A., Wang, Y., Xu, Y., Zhao, G., 2013. Locating South China in Rodinia and Gondwana: a fragment of greater India lithosphere? Geology 41 (8), 903–906. https://doi.org/10.1130/G34395.1.

Cawood, Peter A., Zhao, G.C., Yao, J.L., Wang, W., Xu, Y.J., Wang, Y.J., 2017. Reconstructing South China in phanerozoic and precambrian supercontinents. Earth-Science Reviews 186, 173–194.

Chen, Q., Sun, M., Long, X., Zhao, G., Yuan, C., 2016. U–Pb ages and Hf isotopic record of zircons from the late Neoproterozoic and Silurian–Devonian sedimentary rocks of the western Yangtze Block: implications for its tectonic evolution and continental affinity. Gondwana Research 31, 184–199.

Chen, Z.-H., Zhao, L., Chen, D.-D., Zhao, X.-L., Xing, G.-F., 2017. First discovery of a Palaeoproterozoic A-type granite in southern Wuyishan terrane, Cathaysia Block: evidence from geochronology, geochemistry, and Nd–Hf–O isotopes. International Geology Review 59, 80–93.

Clift, P., Vannucchi, P., 2004. Controls on tectonic accretion versus erosion in sub-duction zones: implications for the origin and recycling of the continental crust. Reviews of Geophysics 42 (2).

Collins, W.J., 2003. Slab pull, mantle convection, and pangaean assembly and dispersal. Earth and Planetary Science Letters 205 (3–4), 225–237.

Collins, Alan S., Pisarevsky, Sergei a, 2005. Amalgamating Eastern Gondwana: The evolution of the circum-Indian orogens. Earth-Science Reviews 71 (3–4), 229–270.

Cui, X., Zhu, W., Fitzsimons, I.C.W., He, J., Lu, Y., Wang, X., Ge, R., Zheng, B., Wu, X., 2015. U–Pb age and Hf isotope composition of detrital zircons from Neo-proterozoic sedimentary units in southern Anhui Province, South China: implications for the provenance, tectonic evolution and glacial history of the eastern Jiangnan Orogen. Precambrian Research 271, 65–82.

DeCelles, P.G., 2000. Tectonic implications of U-Pb Zircon ages of the Himalayan orogenic belt in Nepal. Science 288 (5465), 497–499. https://doi.org/10.1126/science.288.5465.497.

DeCelles, P.G., Ducea, M.N., Kapp, P., Zandt, G., 2009. Cyclicity in Cordilleran orogenic systems. Nature Geoscience 2 (4), 251–257. https://doi.org/10.1038/ngeo469.

Ding, H., Zhang, Z., Dong, X., Yan, R., Lin, Y., Jiang, H., 2015. Cambrian ultrapotassic rhyolites from the Lhasa terrane, south Tibet: evidence for Andean-type magmatism along the northern active margin of Gondwana. Gondwana Research 27, 1616–1629.

Dyck, B., 2016. Textural and Petrological Studies of Anataxis and Melt Transfer in the Himalayan Orogen (D.Phil. thesis). University of Oxford, p. 231.

Gansser, A., 1964. Geology of the Himalayas.:Interscience. Publishers a division of John Wiley, London New York Sydney (tr. Zurich).

Ge, R., Zhu, W., Zheng, B., Wu, H., He, J., Zhu, X., 2012. Early Pan-African magmatism in the Tarim Craton: insights from zircon U–Pb–Lu–Hf isotope and geochemistry of granitoids in the Korla area, NW China. Precambrian Research 212–213, 117–138.

Gehrels, G., Kapp, P., DeCelles, P., Pullen, A., Blakey, R., Weislogel, A., Ding, L., Guynn, J., Martin, A., McQuarrie, N., Yin, A., 2011. Detrital zircon geochronology of pre-Tertiary strata in the Tibetan-Himalayan orogen. Tectonics 30 (5), TC5016. https://doi.org/10.1029/2011TC002868.

Gehrels, G.E., DeCelles, P.G., Ojha, T.P., Upreti, B.N., 2006. Geologic and U-Th-Pb geochronologic evidence for early Paleozoic tectonism in the Kathmandu thrust sheet, central Nepal Himalaya. Geological Society of America Bulletin 118 (1–2), 185–198. https://doi.org/10.1130/B25753.1.

Gürsu, S., Göncüoglu, M.C., 2005. Early cambrian back-arc volcanism in the western Taurides, Turkey: implications for rifting along the Northern Gondwanan Margin. Geological Magazine 142 (5), 617–631.

Guynn, Jerome, Kapp, Paul, Gehrels, George E., Ding, Lin, 2012. U–Pb geochronology of basement rocks in Central Tibet and paleogeographic implications. Journal of Asian Earth Sciences 43 (1), 23–50.

Griffin, W.L., Pearson, N.J., Belousova, E.A., Saeed, A., 2006. Comment: Hf-isotope heterogeneity in zircon 91500. Chemical Geology 233 (3–4), 358–363. https://doi.org/10.1016/j.chemgeo.2006.03.007.

Han, Y., Zhao, G., Cawood, P.A., Sun, M., Eizenhöfer, P.R., Hou, W., Zhang, X., Liu, Q., 2015. Tarim and North China cratons linked to northern Gondwana through switching accretionary tectonics and collisional orogenesis. Geology 44, 95–98.

Hassanzadeh, Jamshid, et al., 2008. U-Pb Zircon geochronology of late neo-proterozoic–early cambrian granitoids in Iran: Implications for paleogeography, magmatism, and exhumation history of Iranian basement. Tectonophysics 451 (1–4), 71–96.

Hawkesworth, C., Cawood, P., Kemp, T., Storey, C., Dhuime, B., Mazur, E., 2009. A matter of preservation. Science 323, 49–50.

Hopkinson, T.N., et al., 2017. The identification and significance of pure sediment-derived granites. Earth and Planetary Science Letters 467.

Horstwood, Matthew S.A., Foster, Gavin L., Parrish, Randall R., Noble, Stephen R., Nowell, Geoff M., 2003. Common-Pb corrected in situ U? Pb accessory mineral geochronology by LA-MC-ICP-MS. Journal of Analytical Atomic Spectrometry 18 (8), 837.

Hu, P., Li, C., Wang, M., Xie, C., Wu, Y., 2013. Cambrian volcanism in the Lhasa terrane, southern Tibet: record of an early Paleozoic Andean-type magmatic arc along the Gondwana proto-Tethyan margin. Journal of Asian Earth Sciences 77, 91–107.

Hu, P., Zhai, Q., Jahn, B., Wang, J., Li, C., Lee, H., Tang, S., 2015. Early Ordovician granites from the South Qiangtang terrane, northern Tibet: implications for the early Paleozoic tectonic evolution along the Gondwanan proto-Tethyan margin. Lithos 220–223, 318–338. https://doi.org/10.1016/j.lithos.2014.12.020.

Huang, X.-L., Xu, Y.-G., Li, X.-H., Li, W.-X., Lan, J.-B., Zhang, H.-H., Liu, Y.-S., Wang, Y.-B., Li, H.-Y., Luo, Z.-Y., Yang, Q.-J., 2008. Petrogenesis and tectonic implications of Neoproterozoic, highly fractionated A-type granites from Mianning, South China. Precambrian Research 165, 190–204. https://doi.org/10.1016/j.precamres.2008.06.010.

Iizuka, T., Campbell, I.H., Allen, C.M., Gill, J.B., Maruyama, S., Makoka, F., 2013a. Evolution of the African continental crust as recorded by U–Pb, Lu–Hf and O isotopes in detrital zircons from modern rivers. Geochimica et Cosmochimi-caActa 107, 96–120. https://doi.org/10.1016/j.gca.2012.12.028.

Iizuka, T., Campbell, I.H., Allen, C.M., Gill, J.B., Maruyama, S., Makoka, F., 2013b. Evolution of the African continental crust as recorded by U–Pb, Lu–Hf and O isotopes in detrital zircons from modern rivers. Geochimica et Cosmochimi-caActa 107, 96–120.

Isozaki, Y., Aoki, K., Nakama, T., Yanai, S., 2010. New insight into a subduction-related orogen: a reappraisal of the geotectonic framework and evolution of the Japanese Islands. Gondwana Research 18 (1), 82–105. https://doi.org/10.1016/j.gr.2010.02.015.

Kaur, P., Zeh, A., Chaudhri, N., Gerdes, A., Okrusch, M., 2011. Archaean to Palaeoproterozoic crustal evolution of the Aravalli mountain range, NW India, and its hinterland: the U–Pb and Hf isotope record of detrital zircon. Precambrian Research 187 (1–2), 155–164. https://doi.org/10.1016/j.precamres.2011.03.005.

Kay, Suzanne Mahlburg, Godoy, Estanislao, Kurtz, Andrew, 2005. Episodic Arc Migration, Crustal Thickening, Subduction Erosion, and Magmatism in the South-Central Andes. Geological Society of America Bulletin 117 (1–2), 67–88.

Keppie, D.F., Currie, C.A., Warren, C., 2009. Subduction erosion modes: Comparing finite element numerical models with the geological record. Earth and Planetary Science Letters 287 (1–2), 241–254. https://doi.org/10.1016/j.epsl.2009.08.009.

Kohn, Matthew J., Paul, Sudip K., Corrie, Stacey L., 2010. The lower lesser Himalayan sequence: a paleoproterozoic arc on the northern margin of the Indian plate. Geological Society of America Bulletin 122 (3–4), 323–335.

Lee, Jeffrey, Whitehouse, Martin J., 2007. Onset of mid-crustal extensional flow in Southern Tibet: evidence from U/Pb zircon ages. Geology 35 (1), 45–48.

Le Fort, P., 1975. Himalayas: the collided range. Present knowledge of the continental arc. American Journal of Science 275, 1–44.

Le Fort, P., 1986. Metamorphism and magmatism during the Himalayan collision. Geological Society, London, Special Publications 19, 159–172.

Li, L.-M., Sun, M., Wang, Y., Xing, G., Zhao, G., Lin, S., Xia, X., Chan, L., Zhang, F., Wong, J., 2011. U–Pb and Hf isotopic study of zircons from migmatisedamphibolites in the Cathaysia Block: implications for the early Paleozoic peak tectonothermal event in Southeastern China. Gondwana Research 19, 191–201.

Li, W.X., Li, X.H., Li, Z.X., 2005. Neoproterozoic bimodal magmatism in the Cathaysia Block of South China and its tectonic significance. Precambrian Research 136, 51–66.

Li, W.X., Li, X.H., Li, Z.X., 2010. Ca. 850 Ma bimodal volcanic rocks in northeastern Jiangxi Province, South China: initial extension during the breakup of Rodinia? American Journal of Science 310, 951–980.

Li, X.-H., Li, Z.-X., He, B., Li, W.-X., Li, Q.-L., Gao, Y., Wang, X.-C., 2012a. The Early Permian active continental margin and crustal growth of the Cathaysia Block: in situ U–Pb, Lu–Hf and O isotope analyses of detrital zircons. Chemical Geology 328, 195–207. https://doi.org/10.1016/j.chemgeo.2011.10.027.

Li, Z.-X., Li, X.-H., Chung, S.-L., Lo, C.-H., Xu, X., Li, W.-X., 2012b. Magmatic switch-on and switch-off along the South China continental margin since the permian: transition from an Andean-type to a Western pacific-type plate boundary. Tectonophysics 532, 271–290.

Li, X.H., Li, W.X., Li, Z.X., Liu, Y., 2008. 850-790 Ma bimodal volcanic and intrusive rocks in northern Zhejiang, South China: a major episode of continental rift magmatism during the breakup of Rodinia. Lithos 102, 341–357.

Long, S., McQuarrie, N., 2010. Placing limits on channel flow: insights from the Bhutan Himalaya. Earth and Planetary Science Letters 290 (3), 375–390.

Long, X., Yuan, C., Sun, M., Kröner, A., Zhao, G., Wilde, S., Hu, A., 2011. Reworking of the Tarim Craton by underplating of mantle plume-derived magmas: Evidence from Neoproterozoic granitoids in the Kuluketage area, NW China. Precambrian Research 187, 1–14.

Martin, A.J., DeCelles, P.G., Gehrels, G.E., Patchett, P.J., Isachsen, C., 2005. Isotopic and structural constraints on the location of the main central thrust in the Annapurna range, central Nepal Himalaya. Geological Society of America Bulletin 117 (7–8), 926–944.

Martin, E.L., Collins, W.J., Kirkland, C.L., 2017. An Australian source for Pacific-Gondwanan zircons: implications for the assembly of northeastern Gondwana. Geology 45, 699–702. https://doi.org/10.1130/G39152.1.

McQuarrie, N., Long, S.P., Tobgay, T., Nesbit, J.N., Gehrels, G., Ducea, M.N., 2013. Documenting basin scale, geometry and provenance through detrital geochemical data: lessons from the Neoproterozoic to Ordovician Lesser, Greater, and Tethyan Himalayan strata of Bhutan. Gondwana Research 23 (4), 1491–1510. https://doi.org/10.1016/j.gr.2012.09.002.

McQuarrie, N., Robinson, D., Long, S., Tobgay, T., Grujic, D., Gehrels, G., Ducea, M., 2008. Preliminary stratigraphic and structural architecture of Bhutan: implications for the along strike architecture of the Himalayan system. Earth and

Planetary Science Letters 272 (1–2), 105–117. https://doi.org/10.1016/j.epsl.2008.04.030.

Merdith, Andrew S., et al., 2017. A full-plate global reconstruction of the neoproterozoic. Gondwana Research.

Morag, N., Avigad, D., Gerdes, A., Harlavan, Y., 2012. 1000–580 Ma crustal evolution in the northern Arabian-Nubian Shield revealed by U–Pb–Hf of detrital zircons from late Neoproterozoic sediments (Elat area, Israel). Precambrian Research 208, 197–212.

Morag, N., Avigad, D., Gerdes, A., Belousova, E., Harlavan, Y., 2011. Crustal evolution and recycling in the northern Arabian-Nubian Shield: New perspectives from zircon Lu–Hf and U–Pb systematics. Precambrian Research 186, 101–116. https://doi.org/10.1016/j.precamres.2011.01.004.

Mottram, C.M., Warren, C.J., Regis, D., Roberts, N.M.W., Harris, N.B.W., Argles, T.W., Parrish, R.R., 2014. Developing an inverted Barrovian sequence; insights from monazite petrochronology. Earth and Planetary Science Letters 403, 418–431. https://doi.org/10.1016/j.epsl.2014.07.006.

Myrow, P.M., et al., 2010. Extraordinary transport and mixing of sediment across Himalayan Central Gondwana during the Cambrian-Ordovician. Geological Society of America Bulletin 122 (9–10), 1660–1670.

Myrow, P.M., Hughes, N.C., McKenzie, N.R., Pelgay, P., Thomson, T.J., Haddad, E.E., Fanning, C.M., 2016. Cambrian– Ordovician orogenesis in Himalayan equatorial Gondwana. Geological Society of America Bulletin. B31507-1.

Myrow, P.M., Hughes, N.C., Paulsen, T.S., Williams, I.S., Thompson, K.R., Bowring, S.A., Peng, S.-C., Ahluwalia, A.D., 2003. Integrated tectonostratigraphic analysis of the Himalaya and implications for its tectonic reconstruction. Earth and Planetary Science Letters 212 (3–4), 433–441. https://doi.org/10.1016/S0012-821X(03)00280-2.

Nowell, G., Parrish, R.R., 2001. Simultaneous acquisition of isotope compositions and parent/daughter ratios by non-isotope dilution-mode Plasma Ionisation Multi-collector Mass Spectrometry (PIMMS). Special Publication-Royal Society of Chemisty 267 (1), 298–310.

Pan, Guitang, et al., 2012. Tectonic evolution of the Qinghai-Tibet Plateau. Journal of Asian Earth Sciences 53, 3–14.

Parrish, R.R., Hodges, V., 1996. Isotopic constraints on the age and provenance of the lesser and greater Himalayan sequences, Nepalese Himalaya. Geological Society of America Bulletin 108 (7), 904–911.

Richards, A., Parrish, R., Harris, N.B.W., Argles, T., Zhang, L., 2006. Correlation of lithotectonic units across the eastern Himalay, Bhutan. Geology 34 (5), 341–344. https://doi.org/10.1130/G22169.1.

Roberts, N.M.W., 2012. Increased loss of continental crust during supercontinent amalgamation. Gondwana Research 21 (4), 994–1000.

Roberts, N.M.W., Spencer, C.J., 2015. The Zircon archive of continent formation through time. Geological Society, London, Special Publications 389 (1), 197–225.

Robinson, D.M., DeCelles, P.G., Patchett, P.J., Garzione, C.N., 2001. The kinematic evolution of the Nepalese Himalaya interpreted from Nd isotopes. Earth and Planetary Science Letters 192 (4), 507–521.

Robinson, F.A., Foden, J.D., Collins, A.S., Payne, J.L., 2014. Arabian Shield magmatic cycles and their relationship with Gondwana assembly: insights from zircon U–Pb and Hf isotopes. Earth and Planetary Science Letters 408, 207–225. https://doi.org/10.1016/j.epsl.2014.10.010.

Scholl, D.W., von Huene, R., 2009. Implications of estimated magmatic additions and recycling losses at the subduction zones of accretionary (Non-collisional) and collisional (Suturing) orogens. Geological Society, London, Special Publications 318 (1), 105–125.

Searle, M.P., Windley, B.F., Coward, M.P., Cooper, D.J.W., Rex, A.J., Rex, D., Tingdong, L., Xuchang, X., Jan, M.Q., Thakur, V.C., 1987. The closing of Tethys and the tectonics of the Himalaya. The Geological Society of America Bulletin 98, 678–701.

Shen, L., Yu, J.-H., O'Reilly, S.Y., Griffin, W.L., Wang, Q., 2016. Widespread Paleoproterozoic basement in the eastern Cathaysia Block: Evidence from metasedimentary rocks of the Pingtan–Dongshan metamorphic belt, in southeastern China. Precambrian Research 285, 91–108.

Shu, L.-S., Faure, M., Yu, J.-H., Jahn, B.-M., 2011. Geochronological and geochemical features of the Cathaysia block (South China): New evidence for the Neoproterozoic breakup of Rodinia. Precambrian Research 187, 263–276. https://doi.org/10.1016/j.precamres.2011.03.003.

Singh, S., Barley, M., Brown, S., Jain, A., Manickavasagam, R., 2002. SHRIMP U–Pb in zircon geochronology of the Chor granitoid: evidence for Neoproterozoic magmatism in the Lesser Himalayan granite belt of NW India. Precambrian Research 118 (3–4), 285–292. https://doi.org/10.1016/S0301-9268(02)00107-9.

Sláma, J., Košler, J., Condon, D.J., Crowley, J.L., Gerdes, A., Hanchar, J.M., Horstwood, M.S.A., Morris, G.A., Nasdala, L., Norberg, N., 2008. Plešovice zircon—a new natural reference material for U–Pb and Hf isotopic micro-analysis. Chemical Geology 249 (1), 1–35.

Song, D., Xiao, W., Han, C., Li, J., Qu, J., Guo, Q., Lin, L., Wang, Z., 2013. Progressive accretionary tectonics of the Beishan orogenic collage, southern Altaids: insights from zircon U–Pb and Hf isotopic data of high-grade complexes. Precambrian Research 227, 368–388.

Spakman, W., Hall, R., 2010. Surface deformation and slab–mantle interaction during Banda arc subduction rollback. Nature Geoscience 3 (8), 562–566. https://doi.org/10.1038/ngeo917.

Spencer, C.J., Cawood, P.A., Hawkesworth, C.J., Prave, A.R., Roberts, N.M.W.W., Horstwood, M.S.A., Whitehouse, M.J., 2015. Generation and preservation of continental crust in the Grenville Orogeny. Geoscience Frontiers 6 (3), 357–372. https://doi.org/10.1016/j.gsf.2014.12.001.

Spencer, C.J., Harris, R.A., Dorais, M.J., 2012a. The metamorphism and exhumation of the Himalayan metamorphic core, eastern Garhwal region, India. Tectonics 31 (1), 1–18. https://doi.org/10.1029/2010TC002853.

Spencer, C.J., Harris, R.A., Dorais, M.J., 2012b. Depositional provenance of the Himalayan metamorphic core of Garhwal region, India: constrained by U-Pb and Hf isotopes in zircons. Gondwana Research 22 (1), 26–35. https://doi.org/10.1016/j.gr.2011.10.004.

Spencer, C.J., Roberts, N.M.W., Santosh, M., 2017a. Growth, destruction, and preservation of Earth's continental crust. Earth-Science Reviews 172. https://doi.org/10.1016/j.earscirev.2017.07.013.

Spencer, C.J., Yakymchuk, C., Ghaznavi, M., 2017b. Visualising data distributions with kernel density estimation and reduced chi-squared statistic. Geoscience Frontiers 8 (6), 1247–1252. https://doi.org/10.1016/j.gsf.2017.05.002.

Stern, C.R., 2011. Subduction erosion: Rates, mechanisms, and its role in arc magmatism and the evolution of the continental crust and mantle. Gondwana Research 20 (2–3), 284–308. https://doi.org/10.1016/j.gr.2011.03.006.

Stern, R.J., Scholl, D.W., 2010. Yin and yang of continental crust creation and destruction by plate tectonic processes. International Geology Review 52 (1), 1–31. https://doi.org/10.1080/00206810903332322.

Su, Yanping, Zhang, Baolin, Zhang, Guoliang, Xu, Xingwang, Liu, Ruilin, 2017. Tectonic settings and geological implications of neoproterozoic Liujiaping VMS deposit, Northwestern Yangtze Block, China. Resource Geology 67 (1), 89–102.

Tate, Garrett W., et al., 2015. Australia going down under: quantifying continental subduction during arc-continent accretion in timor-leste. Geosphere 11 (6), 1860–1883.

Thimm, K.A., Parrish, R.R., Hollister, L.S., Grujic, D., Klepeis, K., Dorji, T., 1999. New U-Pb data from the MCT and lesser and greater Himalayan Sequence in Bhutan. TerrraNosira 2, 155.

Thomas, R.J., Jacobs, J., Horstwood, M.S.A., Ueda, K., Bingen, B., Matola, R., 2010. The Mecubúri and Alto Benfica groups, NE Mozambique: Aids to unravelling ca. 1 and 0.5 Ga events in the east African orogen. Precambrian Research 178, 72–90.

Veevers, J.J., Saeed, A., 2011. Age and composition of Antarctic bedrock re flected by detrital zircons ,erratics, and recycled microfossils in the prydz bay − Wilkes land − Ross Sea − marie byrd land sector (70 ° − 240 ° E). Gondwana Research 20, 710–738. https://doi.org/10.1016/j.gr.2011.03.007.

von Huene, R., Scholl, D.W., 1991. Observations at convergent margins concerning sediment subduction, subduction erosion, and the growth of continental crust. Reviews of Geophysics 29 (3), 279–316.

Wang, J., Li, Z.X., 2003. History of neoproterozoic rift basins in South China: implications for Rodinia break-up. Precambrian Research 122, 141–158.

Wang, J., Shu, L., Santosh, M., 2017. U-Pb and Lu-Hf isotopes of detrital zircon grains from Neoproterozoic sedimentary rocks in the central Jiangnan Orogen, South China: implications for Precambrian crustal evolution. Precambrian Research 294, 175–188.

Wang, J.Q., Shu, L.S., Santosh, M., Xu, Z.Q., 2015. The Pre-Mesozoic crustal evolution of the Cathaysia Block, South China: insights from geological investigation, zircon U–Pb geochronology, Hf isotope and REE geochemistry from the Wugongshan complex. Gondwana Research 28, 225–245.

Wang, Zhilin, et al., 2015b. Detrital zircon U–Pb ages of the proterozoic metaclastic-sedimentary rocks in Hainan Province of South China: new constraints on the depositional time, source area, and tectonic setting of the Shilu Fe–Co–Cu ore district. Journal of Asian Earth Sciences 113, 1143–1161.

Wang, L.-J., Griffin, W.L., Yu, J.-H., O'Reilly, S.Y., 2010a. Precambrian crustal evolution of the Yangtze Block tracked by detrital zircons from Neoproterozoic sedimentary rocks. Precambrian Research 177 (1–2), 131–144. https://doi.org/10.1016/j.precamres.2009.11.008.

Wang, L., Yu, J., O'Reilly, S.Y., Griffin, W.L., Sun, T., Wei, Z., Jiang, S., Shu, L., 2008. Grenvillian orogeny in the Southern Cathaysia Block: constraints from U-Pb ages and Lu-Hf isotopes in zircon from metamorphic basement. Chinese Science Bulletin 53 (19), 3037–3050. https://doi.org/10.1007/s11434-008-0262-0.

Wang, Q., Wyman, D.A., Li, Z.X., Bao, Z.W., Zhao, Z.H., Wang, Y.X., Jian, P., Yang, Y.H., Chen, L.L., 2010b. Petrology, geochronology and geochemistry of ca. 780 Ma A-type granites in South China: petrogenesis and implications for crustal growth during the breakup of the supercontinent Rodinia. Precambrian Research 178, 185–208.

Wang, W., Zhou, M.F., 2012. Sedimentary records of the Yangtze Block (South China) and their correlation with equivalent Neoproterozoic sequences on adjacent continents. Sedimentary Geology 265–266, 126–142.

Wang, X.L., Shu, L.S., Xing, G.F., Zhou, J.C., Tang, M., Shu, X.J., Qi, L., Hu, Y.H., 2012. Post-orogenic extension in the eastern part of the Jiangnan orogen: Evidence from ca 800–760 Ma volcanic rocks. Precambrian Research 222–223, 404–423.

Wang, Y., Xing, X., Cawood, P.A., Lai, S., Xia, X., Fan, W., Liu, H., Zhang, F., 2013a. Petrogenesis of early Paleozoic peraluminous granite in the Sibumasu Block of SW Yunnan and diachronous accretionary orogenesis along the northern margin of Gondwana. Lithos 182–183, 67–85. https://doi.org/10.1016/j.lithos.2013.09.010.

Wang, Y., Zhang, A., Cawood, P.A., Fan, W., Xu, J., Zhang, G., Zhang, Y., 2013b. Geochronological, geochemical and Nd–Hf–Os isotopic fingerprinting of an early Neoproterozoic arc–back-arc system in South China and its accretionary assembly along the margin of Rodinia. Precambrian Research 231, 343–371.

Webb, A.A.G., Yin, A., Harrison, T.M., Célérier, J., Burgess, W.P., 2007. The leading edge of the greater Himalayan crystalline complex revealed in the NW indian Himalaya: implications for the evolution of the Himalayan orogen. Geology 35, 955–958.

Webb, A.A.G., Yin, A., Dubey, C.S., 2013. U-Pb zircon geochronology of major lithologic units in the eastern Himalaya: implications for the origin and assembly of Himalayan rocks. Geological Society of America Bulletin 125 (3–4), 499–522.

Woodhead, J., Hergt, J., Shelley, M., Eggins, S., Kemp, R., 2004. Zircon Hf-isotope analysis with an excimer laser, depth profiling, ablation of complex geometries, and concomitant age estimation. Chemical Geology 209 (1–2), 121–135.

Woodhead, J.D., Hergt, J.M., 2005. A preliminary appraisal of seven natural zircon reference materials for in situ Hf isotope determination. Geostandards and Geoanalytical Research 29 (2), 183–195.

Yakymchuk, C., Brown, C.R., Brown, M., Siddoway, C.S., Fanning, C.M., Korhonen, F.J., 2015. Paleozoic evolution of western marie byrd land, Antarctica. Geological Society of America Bulletin 127, 1464–1484.

Yan, C., Shu, L., Santosh, M., Yao, J., Li, J., Li, C., 2015. The Precambrian tectonic evolution of the western Jiangnan Orogen and western Cathaysia Block: Evidence from detrital zircon age spectra and geochemistry of clastic rocks. Precambrian Research 268, 33–60.

Yao, J., Shu, L., Santosh, M., 2011. Detrital zircon U–Pb geochronology, Hf-isotopes and geochemistry—new clues for the Precambrian crustal evolution of Cathaysia Block, South China. Gondwana Research 20, 553–567.

Yao, J., Shu, L., Cawood, P.A., Li, J., 2016. Delineating and characterizing the boundary of the Cathaysia block and the Jiangnan orogenic belt in South China. Precambrian Research 275, 265–277.

Yao, W.-H., Li, Z.-X., Li, W.-X., Li, X.-H., Yang, J.-H., 2014a. From Rodinia to Gondwaland: a tale of detrital zircon provenance analyses from the southern Nanhua Basin, South China. American Journal of Science 314, 278–313.

Yao, W.H., Li, Z.X., Li, W.X., Su, L., Yang, J.H., 2015. Detrital provenance evolution of the Ediacaran-Silurian Nanhua foreland basin. South China. Gondwana Research 28, 1449–1465.

Yao, W.H., Li, Z.X., Li, W.X., Li, X.H., Yang, J.H., 2014b. From Rodinia to Gondwanaland: a tale from detrital provenance analyses of the Cathaysia block, South China. American Journal of Science 314, 278–313.

Yin, A., Dubey, C.S., Webb, A.A.G., Kelty, T.K., Grove, M., Gehrels, G.E., Burgess, W.P., 2010. Geologic correlation of the Himalayan orogen and Indian craton: Part 1. Structural geology, U-Pb zircon geochronology, and tectonic evolution of the Shillong Plateau and its neighboring regions in NE India. Geological Society of America Bulletin 122 (3–4), 336–359.

Yu, Jin-Hai, et al., 2008. Where was South China in the Rodinia supercontinent?: Evidence from U–Pb geochronology and Hf isotopes of detrital zircons. Precambrian Research 164 (1–2), 1–15.

Yu, J.-H., O'Reilly, S.Y., Wang, L., Griffin, W.L., Zhou, M.-F., Zhang, M., Shu, L., 2010. Components and episodic growth of Precambrian crust in the Cathaysia Block, South China: evidence from U–Pb ages and Hf isotopes of zircons in Neoproterozoic sediments. Precambrian Research 181, 97–114.

Yu, J.-H., O'Reilly, S.Y., Zhou, M.-F., Griffin, W.L., Wang, L., 2012. U–Pb geochronology and Hf–Nd isotopic geochemistry of the Badu Complex, Southeastern China: implications for the Precambrian crustal evolution and paleogeography of the Cathaysia Block. Precambrian Research 222, 424–449.

Yu, J., Zhang, C., O'Reilly, S.Y., Griffin, W.L., Ling, H., Sun, T., Zhou, X., 2017. Basement components of the Xiangshan-Yuhuashan area, South China: defining the boundary between the Yangtze and Cathaysia blocks. Precambrian Research. https://doi.org/10.1016/j.precamres.2017.05.017.

Zhang, S.-H., Zhao, Y., Liu, X.-C., Liu, Y.-S., Hou, K.-J., Li, C.-F., Ye, H., 2012. U–Pb geochronology and geochemistry of the bedrocks and moraine sediments from the Windmill Islands: implications for Proterozoic evolution of East Antarctica. Precambrian Research 206, 52–71.

Zhang, Z.M., Dong, Xin, Santosh, M., Zhao, G.C., 2014. Metamorphism and tectonic evolution of the Lhasa terrane, Central Tibet. Gondwana Research 25 (1), 170–189.

Zhou, J.-C., Wang, X.-L., Qiu, J.-S., 2009. Geochronology of Neoproterozoic mafic rocks and sandstones from northeastern Guizhou, South China: coeval arc magmatism and sedimentation. Precambrian Research 170, 27–42. https://doi.org/10.1016/j.precamres.2008.11.002.

Zhou, M.F., Ma, Y., Yan, D.P., Xia, X., Zhao, J.H., Sun, M., 2006. The Yanbian terrane (Southern Sichuan province, SW China): a Neoproterozoic arc assemblage in the western margin of the Yangtze block. Precambrian Research 144, 19–38.

Zhu, D.-C., Zhao, Z.-D., Niu, Y., Dilek, Y., Wang, Q., Ji, W.-H., Dong, G.-C., Sui, Q.-L., Liu, Y.-S., Yuan, H.-L., 2012. Cambrian bimodal volcanism in the Lhasa Terrane, southern Tibet: record of an early Paleozoic Andean-type magmatic arc in the Australian proto-Tethyan margin. Chemical Geology 328, 290–308.

Zou, Shaohao, et al., 2017. Precambrian continental crust evolution of Hainan Island in South China: constraints from detrital zircon Hf isotopes of metaclastic-sedimentary rocks in the Shilu Fe-Co-Cu ore district. Precambrian Research 296, 195–207.

Zhu, Di-Cheng, et al., 2011. The Lhasa Terrane: record of a microcontinent and its histories of drift and growth. Earth and Planetary Science Letters 301 (1–2), 241–255.